Journal of University of Babylon for Engineering Sciences, Vol. (27), No. (4): 2019.

Improvement of Erosion -Corrosion Resistance of Tin-Bronze Alloy by Addition of Al and Al_2O_3 via Powder Technology

Ali Hubi Haleem **Zuheir Talib khulief** **Zaid Maythem Abbas**

College of Materials Engineering, Babylon University, Babylon, Iraq

alialihhhobi@gmail.com

Submission date:- 24/10/2019	Acceptance date:- 4/12/2019	Publication date:-30/12/2019

Abstract:

The porous (tin-bronze) alloy has many engineering applications, especially in filtration systems, self-lubricating loading chairs and heat exchangers. Because of its unique mechanical and physical properties, it combines light weight, good durability with permeability, thermal and electrical conductivity. In the present study, samples of tin-bronze alloy with chemical composition (90 % Cu, 10 % Sn) have been prepared by using powder metallurgy,(35 wt. %) high purity (99.6 wt. %) NaCl powder was used as a pore-forming agent for the generation of pores, which was subsequently removed by dissolved with water at (100˚C) followed by ultrasonic cleaning (Ultrasonic cleaner device). Aluminum (3%) and alumina (3%, 5%, and 7%) were added to the base alloy to prepare composite samples in addition to the base alloy and study the effect of these additives on physical ,mechanical, corrosion, and erosion -corrosion properties.

The powders were mixed for 5 hours and pressed under 40 MPa. Samples were sintered at(200˚C) for one hour and then the temperature was raised to (600˚C) for period of (180 min) with heating rate (10 ˚C/min) in a vacuum atmosphere (10^{-4} Torr) Then let it cool inside the furnace to room temperature while ensuring continued air discharge. The results showed that the sample of the addition of (3% Al and 7% Al_2O_3,) failed in the sintering process while the rest of the samples succeeded in sintering process under the same conditions.

Several tests were carried out including: microstructure test (light optical microscopy), scanning electron microscopy test (SEM), X-ray diffraction test (XRD), Energy dispersion spectrometer test (EDS), Vickers micro-hardness test ,porosity, density, corrosion behavior (Tafel), and erosion corrosion test. The results of the SEM showed the presence of particle (Al_2O_3) in the matrix of the samples containing the addition of alumina particles. While the results of the X-ray diffraction examination showed that the prepared samples consist of two phases α (Cu, Sn) which represents the alloy matrix and the second phase (ε-Cu_3Sn) as an intermetallic compound. The results of the density and porosity tests showed a decrease in the density value after the addition of aluminum and alumina. This decreasing increases with the increase of the percentage of the addition of alumina, while the porosity increases slightly with the increase of this addition. Through the test of micro-hardness, the results showed that the addition of alumina and aluminum led to an increase in the hardness value, where it was observed to increase the hardness value from (44.41) Hv of the alloy without addition to (83.30Hv) When the percentage of addition was (3% Al+5% Al_2O_3). In corrosion tests, the results of the electrochemical corrosion test (Tafel) in the solution (3.5% NaCl) significantly improved the corrosion resistance as the current density value decreased from (1.76112 µA / mm^2) for base alloy to (0.00326 µA / mm^2) for composite sample of (3%Al) and (5% Al_2O_3). While in the erosion- corrosion test in (3.5% NaCl solution), the rate of erosion corrosion in alloy(90% Cu- 10% Sn) was ($11.5*10^{-4}$ g/hr) and the rate of erosion corrosion for alloy with addition of (3%Al+5%Al_2O_3) was ($5.8*10^{-4}$ g/hr) at steady state condition.

Key words: Tin bronze alloy, Powder metallurgy, Porous structures, Erosion corrosion, Corrosion behavior.

I.0.Introduction

Today porous metallic products are being mass produced for a multitude of applications. A large variety of metals is used, including titanium or super alloys, although bronze and stainless steel meet for most market applications. In general, the production of porous structures consists of various steps: powder fractioning and preparation, compaction or molding, and sintering [1]. Powder metallurgy is the most common method to produce porous metallic products, where the level of porosity, distribution and the size of pores are controlled. Three groups of porous materials produced commercially differ primarily in their porosity style and percentage, these include; metallic filters, self-lubricating equipment's bearings and porous electrodes for batteries and fuel cell [2]. A rigid, permeable structure can be created using powder metallurgy by forming a network of sintered powder particles and interconnected pore channels. Using similar manufacturing equipment and technology as structural powder metallurgy components, porous powder metallurgy materials are normally sintered to densities between 25% and 85% of theoretical mean density [3]. The porosity can be controlled by variation of manufacturing variables such as compaction pressure, sintering temperature and sintering time. It can also be controlled by variation of powder properties such as particle shape, particle size, size distribution, surface texture and other powder characteristics that depend on the material processing method [4]. Materials can be selected from wide varieties depending on the combination of application requirements and economics. The four most common porous metallic materials are bronze, stainless steel, nickel, and nickel-base alloys [5]. In 2011, Iqbal et al, [6]fabricated porous bronze (10% tin-90% Copper)by powder metallurgy technique, the study was focused on the effects of porosity on the mechanical properties, the results showed porosity ranging from 20% to 40%, density (g/cm3) 5.35 – 6.89, compressive strength (MPa) 63 – 150 , an average pore size of 50 – 500 µm , the porosity has significant effects the yield stress and Young's modulus. In 2017, Endah and Sumardiyanto [7] investigate the effect of sintering temperature on the porosity and mechanical properties for a tin bronze product by powder metallurgy ,the study showed that, for 700 ˚C, 750 ˚C and 800 ˚C sintering temperature, porosity values and the rate of wear decreased, but hardness, density and yield strength values increased, while, at temperatures 825 ˚C, 850 ˚C and 900 ˚C, the rate of wear and porosity increased, but hardness, density and yield strength decreased, the density had increased up to 7.08 g/cm3 until a temperature of 800 ˚C while it decreased from 6.80 g/cm3 to 6.27 g/cm3 at temperature of 825-900 ˚C. In 2017 Osama Ihsan, [8] fabricated a porous structure by adding (NaCl) as a pore-forming to tin bronze alloy prepared by powder metallurgy and investigate the physical and mechanical properties of porous sintered tin bronze alloy, the study focused on investigating and optimizing the effect of different parameters of manufacturing condition such as: pore-forming agent (NaCl wt. %), compacting pressure, temperature and sintering duration on the porosity, coefficient of permeability and micro- hardness, the obtain results showed that, an increasing NaCl wt. % and decreasing of compacting pressure, sintering temperature and sintering time leads to increase the ratio of porosity and permeability coefficient but decrease micro-hardness and according to response surface methodology analysis a multi –optimization method based on desirability function used to obtain the optimum process conditions that can be used to manufacturing of porous sintered tin-bronze structure ,these optimum condition were : (35.36 wt.% NaCl),(40 MPa)compacting pressure ,sintering temperature of (193.5C)and sintering time of (180min) to get maximum porosity of (66.32 %),permeability coefficient of (2.96*10-3 cm/min)and micro-hardness of (57.12 Hv). The present study aimed at fabricating a porous structure as filter by adding (NaCl) as a pore-forming to tin-bronze alloy prepared by powder metallurgy and investigate the effect of this addition(3% Al) and different percentage of alumina (3 wt. %, 5 wt. %, and 7 wt. %) on the corrosion behavior and Erosion- corrosion properties."

2.0 Experimental Work:

The samples used in this study were prepared using powder metallurgy method in which the metal powders used (Aluminum, Cupper, Tin, and Alumina), Table (1) shows the purity, Particle size and origin of the used powders.""

2.1. Powder preparation

A wet mixing was carried out in the presence of (2 wt. %) of Ethyl alcohol to reduce the friction and oxidation in the powder particles which results from mixing process. A mixture of (90 wt. %Cu-10 wt. %Sn) was prepared and then it was added 35 wt. % NaCl (pore-forming agent) to prepared base alloy (A) followed by adding 3% of (Al) and different percentages of Al2O3 (3%, 5%, 7%) to prepared composite alloys (B, C, D) as shown in the table (2). The mixing process was achieved by ball mill,

type (STGQM-15/-2) for 5 hours in order to get the perfect and homogeneous distribution of powder particle. The mixture was dried at 60 ˚C for 30 min.”"

2.2 Compaction of Powder

The steel die used in samples preparation process was cylindrical one direction action dies with diameters (13) mm. The samples were prepared as disk shape with (13 mm) in diameter and (8 mm) in height as shown in the figure (1).The applied stress is (40MPa) on the metallic powders in order to get green compacting samples by using electrical-hydraulic press one channel device, type CT340-CT440. A constant loading rate of (0.3) KN/sec was used for all compacting processes with a duration of 8 min. for the achieved pressure, the inside walls of the steel die were lubricated by graphite.”

2.3 Sintering Process

The sintering process of the green compacts was achieved under vacuum conditions by using vacuum tube furnace type MTI-(GSL1600X). A pressure of (10^{-4} torr) was used. The samples sintering process included the following as shown in the figure (2):

- Heating from room temperature to (200 ˚C) and soaking for (60) min with heat rate (10 ˚C/min).
- Heating from (200 ˚C) to (600 ˚C) and soaking for 180 min with heat rate (10 ˚C/min).
- Slow cooling in the furnace with continuing vacuum to room temperature.

It was observed after sintering process that the sample (D) with addition of (3% Al and 7% Al_2O_3) had failed after the sintering process. The reason of the failure may be because of increasing in the proportion of (Al_2O_3) to (7%) lead to obstacles the sintering process and prevent the interaction between copper and tin to form solid solution (α) or intermetallic compound (Cu_3Sn) and increase in space between copper and tin.

2.4 Removing of the Space Holder

The sintered samples were immersed in a distilled water by electro-magnetic stirrer type [STR-700 MD] for (7 hrs.) at (100˚C) and also complete the process by using Ultrasonic-cleaner, type VGT-1860QTD-42 KHz) for removing and dissolving particle of NaCl. Figure (3) shows some samples prepared after this process.”

2.5 Testes of Samples:

2.5.1 Microstructure Characterizer and Chemical Analysis

2.5.1.1. Optical Microscope test

"Sintered samples were ground by using SiC paper grits as (400, 800, 1200 and 2000) then polished by using diamond solution. The samples were etched by (5g FeCl3 + 3 ml HCL + 92 ml distilled water) at room temperature [8]. After etching, the samples were washed with distilled water and dried by using an electric drier. An optical microscope type Olympus microscope manufactured by Japan with suitable magnification was used to capture the microstructure of the samples."

2.5.1.2 Scanning Electron Microscopy (SEM) and (EDS) Analysis

In this study, SEM images were captured in order to investigate the microstructure clearly with high accuracy, characterize the morphology of the surface, porosity, and size of pores. While chemical composition was analyzed by (ESD). The samples were ground with appropriate grinding papers, and then etched as the same followed procedure in optical microscopy test. This test was achieved at university of Babylon /pharmacy college labs. Using scanning electron microscope devise type (FEL, Quanta 450)."”

2.5.2 Characterization Test

2.5.2.1 X-Ray Diffraction Analysis (XRD)

Two samples were prepared after sintering and removing pore-forming agent to the XRD testing first sample was the base alloy (A) with 90 wt.% Cu and 10 wt.% Sn .and the second sample was (C)

that have the addition of 3 wt.% (Al) and 5 wt.% (Al_2O_3). The X ray diffracting was used in order to determine the phases produced after sintering and compare it with standard charts.

2.5.3 Physical Tests

2.5.3.1 Porosity and Density Test

The density and porosity of sintered samples were measured according to ASTM B-328 as follows [9]:

- After drying at 100˚C for 5 hours in vacuum furnace at a pressure of (10^{-4} torr) the sample was weighted, and the weight represent mass (A).
- At room temperature, the sample is completely immersed in oil with a density of (0.8 g/cm^3) for 30 min.
- Weighting the fully impregnated sample in air, to get the mass B.
- Weighting the fully impregnated sample in water, to get the mass C.

The density and porosity have been calculated by the following equations [7]:

$$\mathbf{P = \left[\frac{B-C}{D_o(B-c)}\ X\ 100\right] D_w} \quad \text{(3.1)}$$

$$\mathbf{D = \left[\frac{A}{D_o(B-c)}\right] D_w} \quad \text{(3.2)}$$

Where:

$\mathbf{D_o}$ = density of oil (0.8 g/cm^3)

$\mathbf{D_w}$ =density of water (1 g/cm^3)

2.5.4 Mechanical Test

2.5.4.1 Micro-Hardness Test

Appropriate polishing was achieved before subjecting the samples to the test. The test was achieved to the sintered samples (13mm) in diameter and (8mm) in height. The test was conducted at micro Vickers hardness devise type (digital micro Vickers hardness tester TH 717) according to ASTM E384 using a load of (300g) for (10sec) the hardness was recorded as an average of six reading for each sample."

2.5.5 Corrosion Tests:

2.5.5.1 Electrochemical test

Polarization technique for corrosion behavior used to observe the anodic and cathodic behaviors in another word monitoring the corrosion reactions on samples of desired metal. Electrochemical tests were performed by Potentiostatic type (winking M lab 200, Germany) according to the American society for testing and materials (ASTM). The counter electrode was Pt electrode, the reference electrode was SCE and working electrode (sample) according to the American society for testing and materials (ASTM).The corrosion resistance of the samples (A, B, and C) were studied in a solution of 3.5% NaCl and distilled water at room temperature.. Corrosion current density measurement is obtained by using the following equation (1) [10]:

$$\mathbf{i = \frac{I\ cor}{A}} \quad \text{1}$$

Where:

i = corrosion current density, μA/cm^2,

Icor = total corrosion current, μA, and

A = exposed SAMPLE area, cm^2.

2.5.5.2 Erosion/Corrosion Test

Erosion is a mechanical wear process in other words, loss of materials from solid surfaces by the impingement or impacting of liquid, gases or solids. The erosion-corrosion testing device was designed and manufactured according to (G 73) ASTM. The erosion-corrosion device consists of glass tank, motor, tubes to project a solution of 3.5% NaCl at room temperature on the sample through nozzle. A solution of 3.5% NaCl at room temperature which caused erosion - corrosion is projected to fall at 90˚, from the nozzle and with speed of (1.12 m/s). The nozzle is (1 mm) in diameter and positioned at a fixed distance of (10 mm) from the sample."

3.0. Results and discussion:

Optical microscope was used to obtain the microstructure of the etched alloys (A, B, C). It is observed that the alloys after sintering process have a microstructure of bright regions which represent α-phase network matrix of the microstructure, and the other region is dark which refers to as fine ε(Cu3Sn)-phase (intermetallic compound) for base alloy and these results are in agreement with [8],while particles of (Al2O3) in the matrix of alloys (B) and (C) as showed in figures (4) to (6).

The mechanical and physical properties of tin-bronze alloy are significantly affected by the microstructure. So, through using scanning electron microscope (SEM) in order to examine the microstructure of two alloys (A, C), it was noted that alloy (A) had a microstructure of dark region represent α (Cu, Sn)-phase as the matrix of the alloy and bright region of (ε-Cu3Sn) as intermetallic compound, while the sample (C) had a microstructure of dark region represent α (Cu, Sn)-phase, bright region of (ε-Cu3Sn) as intermetallic compound and particles of Al2O3 in the matrix of alloy. Red arrows refer to the particles of Al2O3. as shown in figure (7) and figure (8).These results confirmed by the chemical composition analysis (EDS) Where the appearance of oxygen and aluminum are observed in sample (C) with additions of (Al and Al2O3) and not observed in sample (A) without this additions as shown in figures (9) and (10).

Figure (11) shows (XRD) pattern for a base metal (A). Figure (12) shows (XRD) pattern for sample (C) that has addition of (3% Al and 5% Al2O3). The XRD results of the alloys insure the presence of two phases, α (Cu, Sn)-phase as a matrix of the alloy, and ε – (Cu3Sn) as intermetallic phase and these results are in agreement with [8]. There was no indication that aluminum oxide particles were present because they were outside the X-ray detection limits

Table (3) shows the values of the experimental porosity and density measured for alloys (A, B, C). As can be seen, the density of alloys (B, C) is lower than base alloy (A), while the porosity is larger than base metal. This is because the addition of aluminum oxide and aluminum, which have a density less than the density of copper and tin was at the expense of the proportion of copper and tin, the density of aluminum oxide and aluminum is (3.69 g/cm3), (2.7 g/cm3) respectively, while the density of copper and tin is (8.9 g/cm3), (7.3 g/cm3) respectively [9]. On the other hand, increasing in the proportion of the addition of Al2O3 in samples (B, C) acting as barrier between copper and tin from interaction through the sintering process and this leads to an increase in the porosity and decrease in density.

Hardness of the examined samples is shown in Table (4). Hardness of a material depends on many factors such as microstructure, type of material and alloying elements. Since plastic deformation in crystals is caused by the motion of dislocations, any obstacle to dislocation motion will hinder deformation as the result the grain strengthened [11]. As can be seen that the added particles of (Al2O3) lead to increase hardness, due to strengthening which is a mechanism caused by (Al2O3) particles. These particles tend to restraint movement of the matrix phase in the vicinity of each particle; the matrix transfers some of the applied stress to the particles, which bear a fraction of the load [12]. The strengthening effect results from the role of these particles as obstacle dislocation motion. These particles form incoherent interface with the matrix, a wide number of dislocations are created at the interface, so material becomes strengthened [13, 14].

Polarization curves for alloys (A, B, and C) are illustrated in figures (13) to (15) respectively. Test was conducted with solution of 3.5% NaCl to understand the corrosion behavior in such environments. Corrosion parameters observed from these curves (E cor, I cor) and current density are listed in Table (5). However, the corrosion currents of all samples were determined by electrochemical method. As can be seen the corrosion current of the base alloy (A) in the solution of 3.5% NaCl was (233.64 μA), while the corrosion current of sample (B) and (C) is (0.94311 μA) and (0.43356 μA) respectively in the same solution. As we noted the addition of (Al) and (Al2O3) improve the corrosion

resistance. Table (4.5) shows the current density of samples decreased from (1.76112 μA/mm2)for base alloy (A) to (0.00326 μA /mm2) with addition of (3%Al) and (5%Al2O3) in (Cu-Sn) matrix due to increase passive behavior of this addition. Thus related to role of Al to form a passive film on the surface of the alloys, the Passive film increase the corrosion resistance of the alloy compare with base alloy (A).

Figure (16) shows the results erosion-corrosion rates in quiescent 3.5% NaCl solution with time of alloys (A, B, and C) after exposure times for (10 hrs.) at 0.5 hr cycle using impact angle 90º. At first time of expose to corrosive solution, the erosion corrosion rate is expected to be higher because of easy removal of corrosion product and occurrence of fresh metal surface to contact of corrosive media [15]. In the first stage (incubation period) the surface of the sample was subjected to (deformation) due to impingements of water jet. The second period represents the acceleration part due to cracking and spalling of the hardened surface by fatigue mechanism, because of strain hardening. These two stages were followed by slowing region. The cause of reducing of erosion corrosion rate is due to the formation of grooves on the surface of the sample which then filled with water. Hence, water in these grooves absorbs the impact energy of the water jet [16]. As can be seen in figure (16) the erosion-corrosion rate decreased when the base alloy was alloyed and strengthen with (Al) and (Al2O3). This addition decreased the corrosion current, and increased the hardness which resists the wearing of the surface. The presence of sites of large pits at the surface of base alloy exposed to 3.5%NaCl solution is higher than that of alloys (B, C) .This is attributed to high chloride ion contents and low pH inside the pit tend to accelerate the anodic dissolution reaction within the pits which leads to growing pits and increasing the corrosion rate of alloy. This is consistent with results of the researcher Zahair et al [17]. It can be seen that the corrosion rates of all samples increased as the expose time increased and then attained stable values. This is attributed to the patina film which was formed on the surface of the Tin-bronze alloy. The addition of (Al) to Tin-bronze reduced the selective leaching behavior and helps building a protective oxide rich in Al2O3."

4.0 Conclusions

1. The sample (A) (90 % Cu, 10 % Sn) prepared with condition of [compacting pressure (40) MPa, Sinter temperature (600 ℃) for period (180) min], have a microstructure consisting of two phases α (Cu, Sn) phase as the matrix of the alloy and (ε-Cu_3Sn) as intermetallic phase.
2. The samples (B, C) with the addition of (3% Al, 3% Al_2O_3) and (3% Al, 5% Al_2O_3) respectively. At the same condition of sample (A), have a microstructure consisting of phases α (Cu, Sn) phase as the matrix of the alloy, ε-(Cu_3Sn) as intermetallic phase and particles of Al_2O_3 in the matrix of alloy.
3. The sample (D) that had the addition of (3% Al, 7% Al_2O_3) failed in sintering conditions.
4. Addition of (3% and 5% Al_2O_3 particle) to base alloy improves mechanical properties as micro hardness was increased from (44.41) HV for base alloy to (66.34) HV and (83.3) HV for samples B, C respectively.
5. Addition of (3%Al) and (5% Al_2O_3) reduced the current density from (1.76112 μA/mm^2) for sample A to (0.00711 μA/mm^2) and (0.00326 μA/mm^2) for samples B and C respectively.
6. The erosion corrosion rate for alloy (B, C) are ($7.94*10^{-4}$ g/hr) and ($5.83*10^{-4}$g/hr) respectively, is lower than base alloy A with erosion corrosion rate ($11.54*10^{-5}$ g/hr) at the steady state conditions.
7. The density of samples (B, C) are (4.79 g/cm^3) and (4.68 g/cm^3) respectively, is lower than of base alloy (A) (4.91 g/cm^3), while the porosity of samples (A, B) is (60.12%)and (64.54%) respectively, which is more than of base alloy (A) (57.33%).

CONFLICT OF INTERESTS.

- There are no conflicts of interest.

5.0. References

[1] P. Neumann, Metal foams and porous metal structures. In: J. Banhart, M.F. Ashby, N. A. Fleck, editors. Int. Conf., Bremen, Germany, 14–16 June. Bremen: MIT Press–Verlag, 1999. p. 167.

[2] M. Can, A. B. Etemoglu, International Journal of Powder Metallurgy, 17, 2004, pp. 340–349.

[3] M. Eisenmann, Porous P⁄M technology, in: ASM HandBook, 17, 2000.

[4] D. Poquillon, J. Lemaitre, V. Baco-Carles, Ph. Tailhades, J. Lacaze, Journal of Powder Technology, 126, 2002, 65–74.

[5] L. Albano-Muler, International Journal of Powder Metallurgy, 14, 1982, p. 2.

[6] N. Igbal, P. Xue. H. J. Liaoa, B. Wangb, Y.L. Li, 'Material characterization of porous bronze at high strain rates' , journal of materials science and Engineering , No,528 , 2011, pp.4408-4412.

[7] S. E. Susilowati and D. Sumardiyanto, 'Effect of sintering temperature on the mechanical Properties for a Cu-Sn-C Alloy product by powder metallurgy' international journal of Metallurgy Engineering, vol.6, No 1 , 2017, pp.10-17.

[8] O. I. Ali. "Investigation the parameters Affecting the fabrication of porous metal by p/m". M.S. thesis, Univ. of Babylon, Babil, Iraq, 2017.

[9] ASTM B-328, "Standard Test Method for Density, Oil Content, and Interconnected Porosity of Sintered Metal Structural Part and Oil – Impregnated Bearing "ASTM international. 2003.

[10] Designation: G 102 – 89, "Calculation of corrosion rates and related information from electrochemical measurements", American society for testing and materials, copyright ASTM, 1994.

[11] O. Ajaja, "Material science and Engineering, lamlad Publications", Ado - Ekiti ,Nigeria, p 108, 2014.

[12] R. J. Jenix, D. Chandramohan, K.S. Sucitharan, 'An Overview on Development of Aluminium Metal Matrix Composites with Hybrid Reinforcement', International Journal of Science and Research (IJSR), India, Vol. 1, No. 3, 2012, pp. 2319- 7064.

[13] Nikhilesh Chawla, Yu-Lin Shen, 'Mechanical Behavior of Particle Reinforced Metal Matrix Composites', Advanced Engineering Materials, Vol. 3, No. 6, 2001, pp. 357-370.

[14] M. A. Meyers, K. K. Chawla, Mechanical Behavior of Materials, Sixth ed., Cambridge University. 2009

[15] Z. Brodarac, Z. P. Mrvar, J. Medved, and P. Fajfar ,"Local Squeezing Casting Influence on The Compactness of AlSi10Mg Alloy Casting", Metalurgija,Metabk, Vol.46, No.1, 2007, pp.29-35.

[16] [16] T. McGuinnes and A. Thiruvengadam**,** ASTM Erosion, wear and interface with corrosion, pp. (30-50), 1973.

[17] M. Z. Gasem and A. M. Al-Qutub, Corrosion Behavior of Powder Metallurgy Aluminum Alloy 6061/ Al2O3 Metal Matrix Composites", The 6th Saudi Engineering Conference, KFUPM, Dhahran, Vol**.5,** December 2002, pp271-280.

Table (1): The purity and the Average Particle Size of the Powder Used.

powder	Purity%	Average particle size(µm)	Company or supplier
Cu	99.9	22.93	Central Drug House (p) Ltd/ India
Sn	99.6	22.56	Central Drug House (p) Ltd/ India
Al_2O_3	99.7	12.90	Central Drug House (p) Ltd/ India
Al	99.6	21.14	Central Drug House (p) Ltd/ India

Table (2): Prepared Samples.

Samples code	The mixed powder of (90% Cu-10% Sn)%	Al %	Al_2O_3 %	NaCl %
Base alloy (A)	65	——	——	35
B	59	3	3	35
C	57	3	5	35
D	55	3	7	35

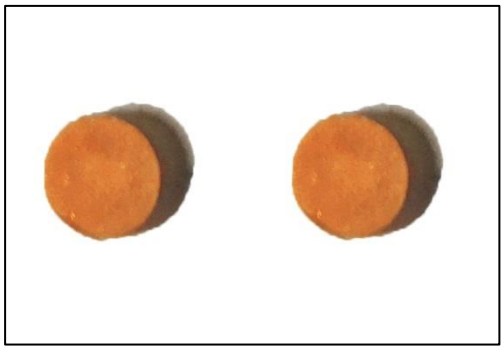

Figure (1): Some of Prepared Samples.

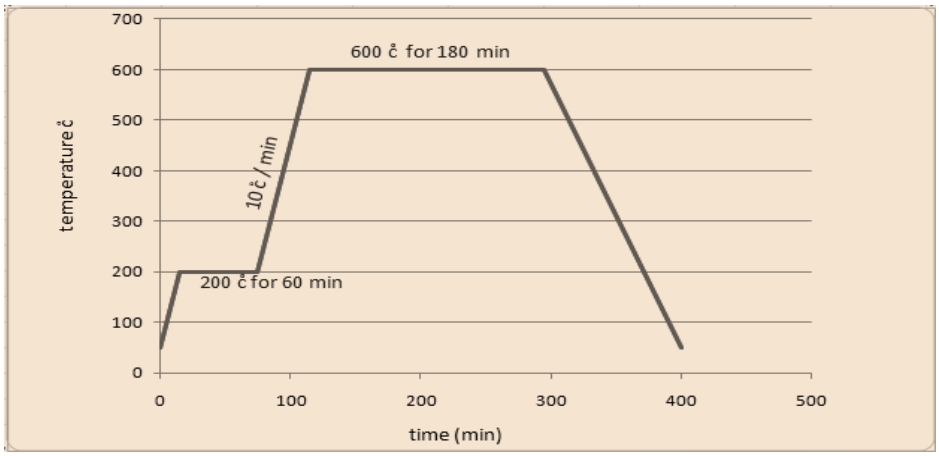

Figure (2): The Sintering Program of the Green Samples.

Figure (3): The Samples Prepared After Removing NaCl.

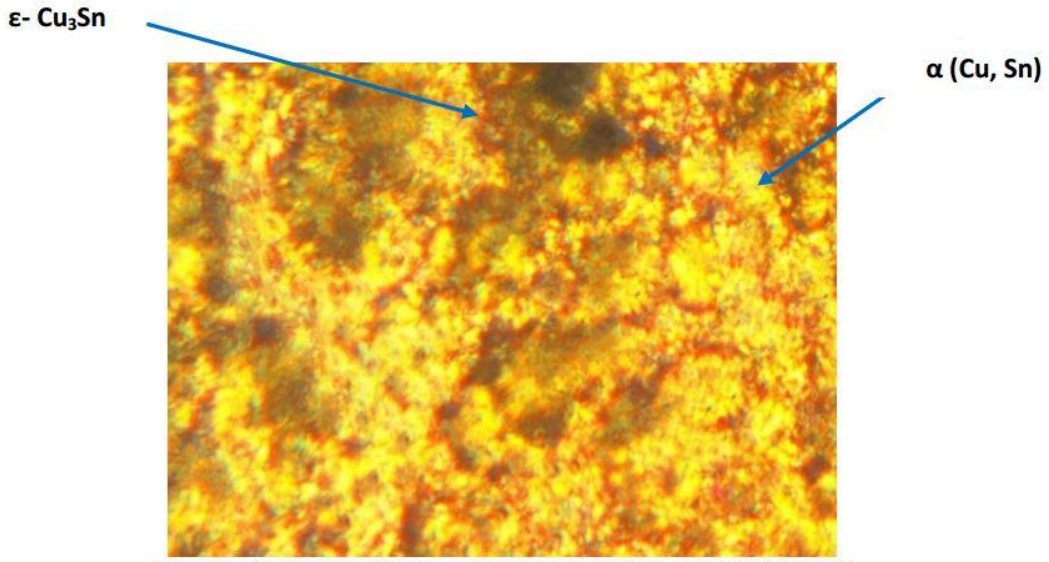

Figure (4): Optical Microscope Image of Base alloy (A) (600X)

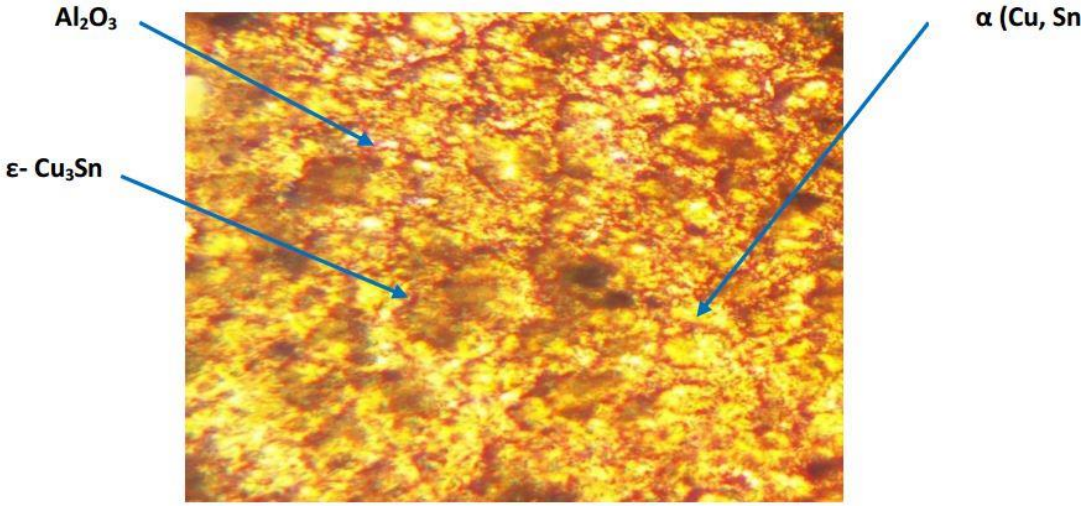

Figure (5): Optical Microscope Image of Alloy (B) (600X).

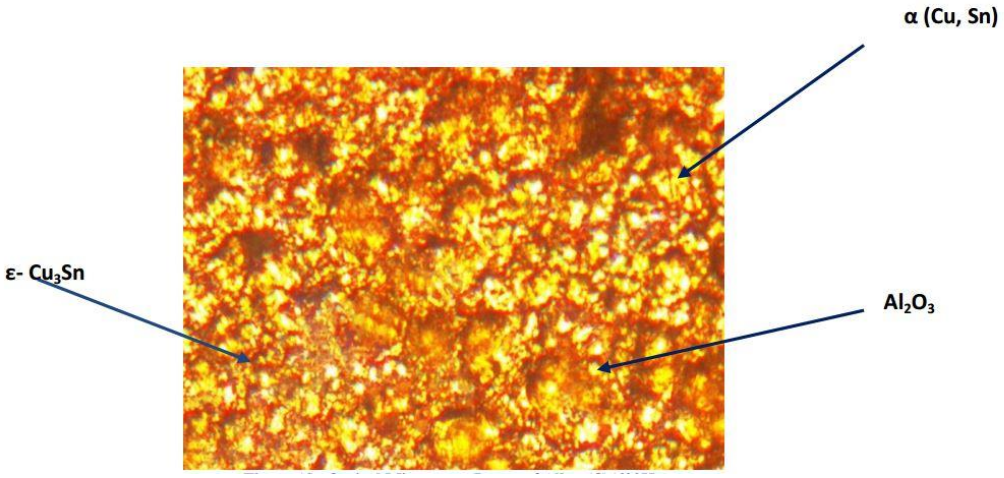

Figure (6): Optical Microscope Image of Alloy (C) (600X).

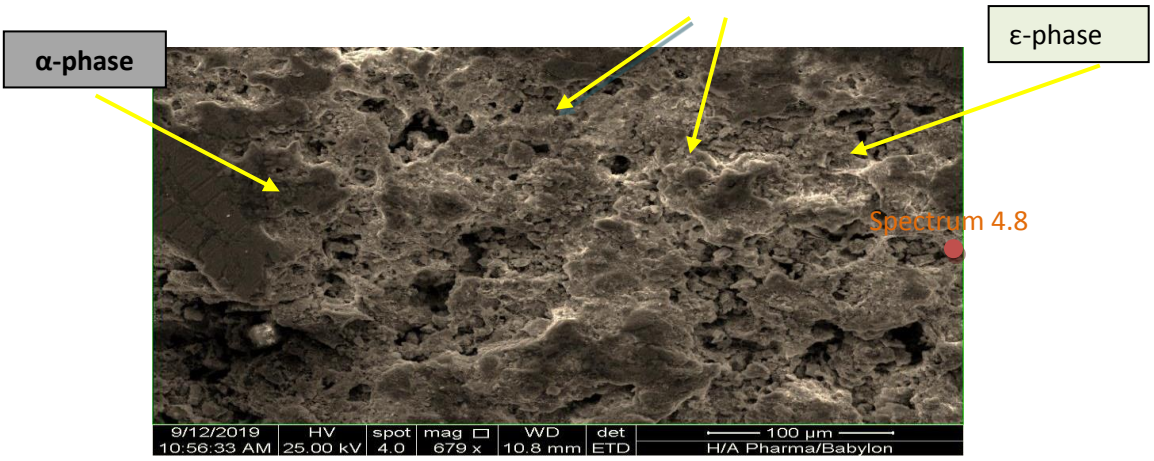

Figure (7): SEM-Image Represent Morphology of Base Alloy (A).

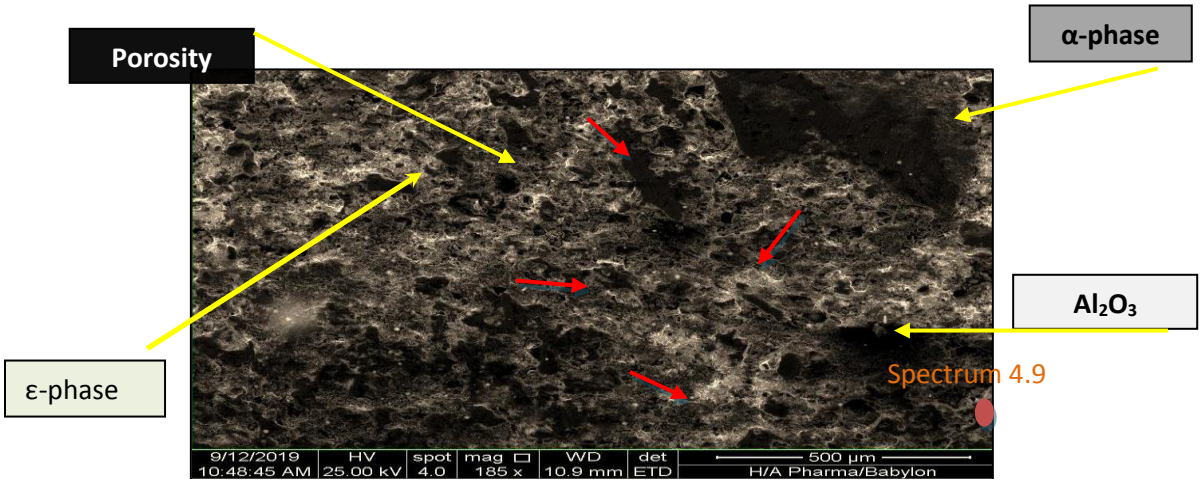

Figure (8): SEM-Image represents Morphology of Alloy(C).

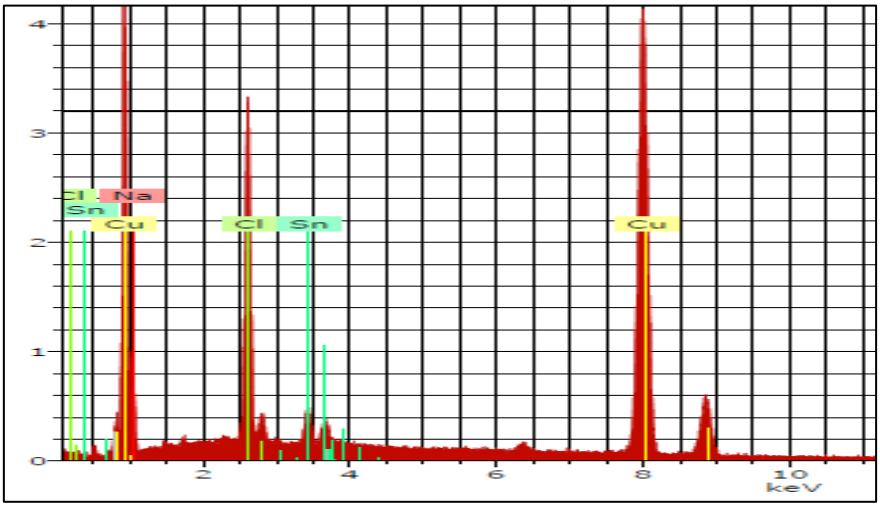

Figure (9): EDS Analysis results for Base alloy (A).

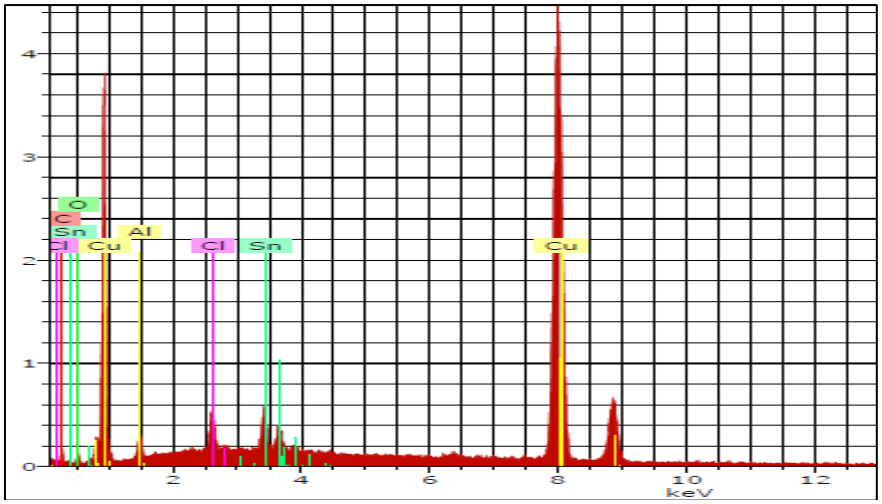

Figure (10): EDS Analysis results for Alloy (C).

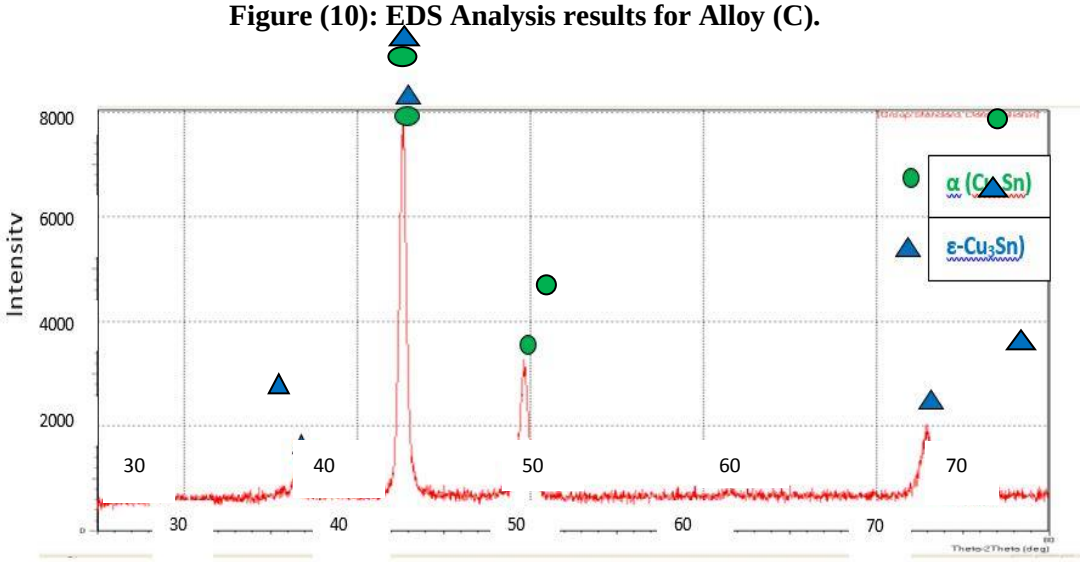

Figure (11): XRD Pattern Analysis for Base Alloy (A).

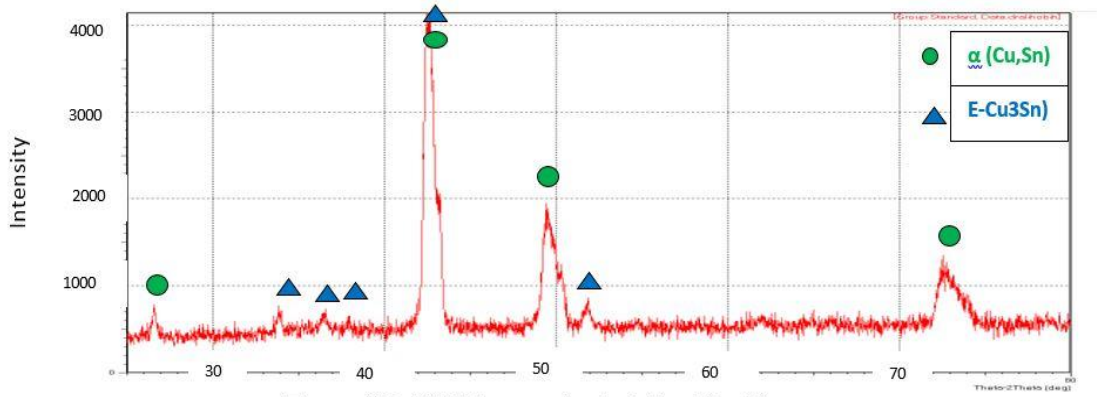

Figure (12): XRD Pattern Analysis for Alloy(C).

Table (3): The Values of Densities and Porosity of Prepared Alloys.

Alloy Code	Density(g/cm^3)	Porosity %
Base alloy (A)	4.91	57.33
B	4.79	60.12
C	4.68	64.54

Table (4): The Hardness of the Examined Samples.

Alloy code	Vickers Hardness(HV) g/mm^2
A(Base alloy)	44.41
B	66.34
C	83.3

Table (5): Corrosion Parameters (E cor, I cor and Current Density).

Alloys Code	E cor.(mV)	I cor. (µA)	Current density µA/mm^2
A	-266.9	233.64	1.76112
B	-380	0.94311	0.00711
C	-356.3	0.43356	0.00326

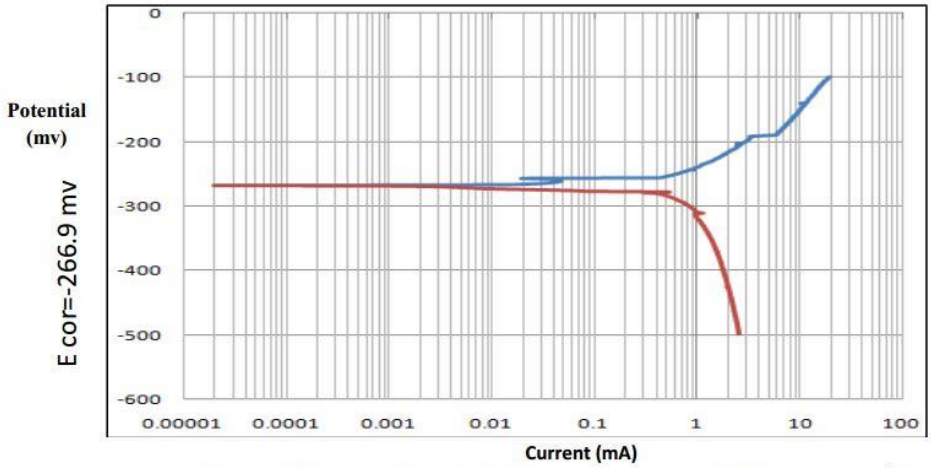

Figure (13) Potentiostatic Polarization curve of alloy (A). I cor=233.64 µA

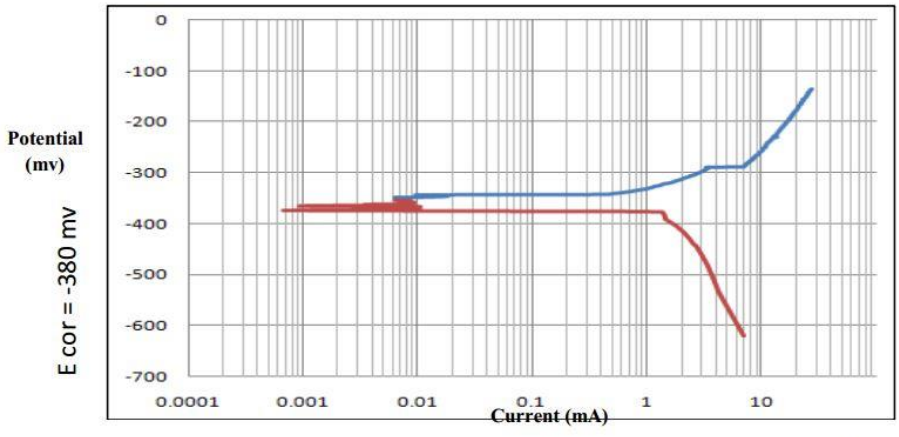

I cor = 0.9411 µA

Figure (14): Potentiostatic Polarization curve of alloy (B).

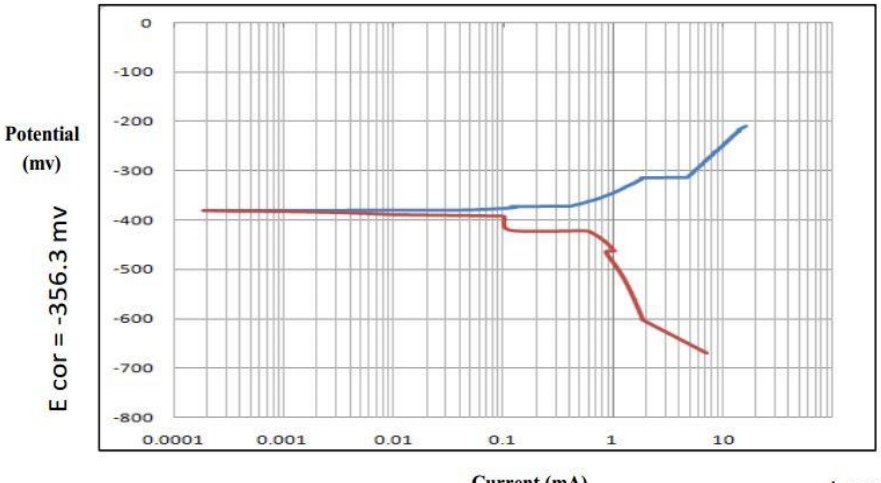

Figure (15): Potentiostatic Polarization curve of sample(C). I cor = 0.43356 µA

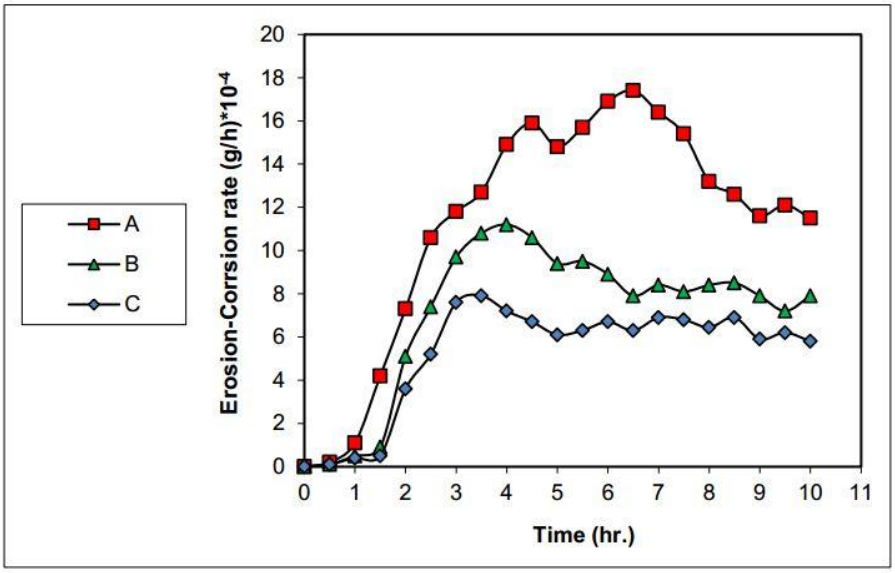

Figure (16): Erosion –corrosion rate versus time when using 3.5%NaCl

تحسين مقاومة التآكل لسبيكة نحاس– قصدير بإضافة الالمنيوم واوكسيد الالمنيوم بواسطة تكنلوجيا المساحيق

علي هوبي حليم زهير طالب خليف زيد ميثم عباس

كلية هندسة المواد، جامعة بابل، بابل، العراق

alialihhhobi@gmail.com

الخلاصة

سبيكة (قصدير–– برونز) ذات التركيب المسامي تمتلك العديد من التطبيقات الهندسية ولاسيما في انظمة الترشيح، كراسي التحميل ذاتية التزييت، المبادلات الحرارية. لكونها تمتاز بخصائص ميكانيكيه وفيزيائية فريدة حيث تجمع ما بين خفة الوزن والمتانة الجيدة مع القدرة على النفاذية والتوصيل الحراري والكهربائي. في العمل الحالي تم تحضير نماذج من سبيكة (قصدير–– برونز) ذات التركيب الكيمائي (90 wt. % Cu, 10 wt. % Sn) بتقنية ميتالورجيا المساحيق، وتم استخدام دقائق مسحوق (NaCl) عالية النقاوة (99.6 wt. %) كعامل لتوليد المسامات وبنسبة اضافة (35 wt. %) والتي تم ازالتها لاحقا عن طريق اذابتها بالماء عند درجة (100˚C) تبعتها عمليه تنظيف باستعمال جهاز الموجات فوق الصوتية (Ultrasonic cleaner device). تم اضافة كلا من الالمنيوم بنسبة (3 wt. %) واوكسيد الالمنيوم بثلاث نسب مختلفة (3% 5%,7%,) الى السبيكة الاساس ذات التركيب الكيميائي (90% Cu, 10% Sn) لتحضير عينات متراكبة اضافة الى العينة الاساس ودراسة تأثير هذه الاضافات على السلوك الفيزيائي والميكانيكي والتاكلي والتاكل بالتعرية.

خلطت المساحيق لمدة (5) ساعات وكبست تحت ضغط (40 MPa) وتم تلبيد العينات عند درجة حرارة (600˚C) ولفترة زمنية (180 min) بعد ان تركت ساعة واحدة عند درجة حرارة (200˚C) في جو مفرغ من الهواء ولغاية (10^{-4} Torr) ثم تركت العينات لتبرد داخل الفرن الى درجة حرارة الغرفة مع ضمان استمرار تفريغ الهواء. اظهرت النتائج فشل العينة ذات الإضافة (7 wt. % Al_2O_3, 3 wt. % Al) في عمليه التلبيد في حين نجحت بقية العينات في عمليه التلبيد تحت نفس الظروف.

اجريت العديد من الاختبارات وتضمنت: فحص البنيية المجهرية (المجهر الضوئي)، اختبار البنية (المجهر الإلكتروني)، فحص التحليل الكيمائي (EDS)، اختبار حيود الأشعة السينية (اشعة اكس)، المسامية، الكثافة، اختبار الصلادة الميكروية (فيكرز)، فحص التآكل (تافل)، وفحص تآكل بالتعرية. اظهرت نتائج المجهر الالكتروني وجود دقائق (Al_2O_3) في ارضية العينات المضاف اليها دقائق اوكسيد الالمنيوم. بينما اظهرت نتائج فحص حيود الأشعة السينية ان العينات المحضرة تتكون من طورين هما α(Cu,Sn) الذي يمثل ارضية السبيكة الاساس والطور الثاني (ε-Cu_3Sn) كمركب شبه معدني. كما اظهرت نتائج فحص الكثافة والمسامية انخفاض في قيمة الكثافة بعد اضافة الالمنيوم واوكسيد الالمنيوم ويزداد هذا الانخفاض مع زيادة نسبة اضافة اوكسيد الالمنيوم في حين تزداد المسامية بنسبة قليل مع زيادة هذه الاضافة. من خلال اختبار الصلادة الدقيقة بينت النتائج ان اضافه اوكسيد الالمنيوم والالمنيوم أدت الى زيادة في قيمه الصلادة حيث لوحظ زيادة قيمه الصلادة من (44.41 HV) للسبيكة الاساس الى (83.3HV) عند اضافة 3%Al واوكسيد الالمنيوم (7%). اما في اختبارات التآكل، فقد اشارت نتائج فحص التآكل الكهروكيميائية (تافل) في محلول (3.5 wt. %NaCl) تحسن كبير في مقاومة التآكل حيث لوحظ انخفاض في قيمة كثافة التيار من ($1.76112\mu A/mm^2$) للسبيكة الخالية من اضافة الالمنيوم واوكسيد الالمنيوم الى ($0.00326\ \mu A/mm^2$) للسبيكة بعد اضافه الالمنيوم (3 wt.% Al) واوكسيد الالمنيوم بنسبة (5 wt. %). ومن خلال اختبار التآكل بالتعرية في محلول (3.5 wt. %NaCl) لوحظ ان معدل التاكل بالتعرية بعد اضافة3% الالمنيوم و5% واوكسيد الالمنيوم كان ($5.8*10^{-4}$ g/hr.) في حين بلغ معدل التاكل بالتعرية للنموذج بدون اضافة الالمنيوم واوكسيد الالمنيوم ($11.5*10^{-4}$ g/hr) عند المنطقة المستقرة.